# IMMUNE SYSTEM APPLICATIONS OF STRUCTURE-AIDED DRUG DESIGN

*Acta Cryst.* (1995). D**51**, 511–521

## Comparative X-ray Structures of the Major Binding Protein for the Immunosuppressant FK506 (Tacrolimus) in Unliganded Form and in Complex with FK506 and Rapamycin

BY KEITH P. WILSON, MASON M. YAMASHITA, MICHAEL D. SINTCHAK, SERGIO H. ROTSTEIN, MARK A. MURCKO, JOSHUA BOGER, JOHN A. THOMSON, MATTHEW J. FITZGIBBON, JAMES R. BLACK AND MANUEL A. NAVIA*

*Vertex Pharmaceuticals Incorporated, 40 Allston Street, Cambridge, MA* 02139-4211, *USA*

(*Received* 21 *July* 1994; *accepted* 12 *December* 1994)

### Abstract

FK506 (tacrolimus) is a natural product now approved in the US and Japan for organ transplantation. FK506, in complex with its 12 kDa cytosolic receptor (FKBP12), is a potent agonist of immunosuppression through the inhibition of the phosphatase activity of calcineurin. Rapamycin (sirolimus), which is itself an immunosuppressant by a different mechanism, completes with FK506 for binding to FKBP12 and thereby acts as an antagonist of calcineurin inhibition. We have solved the X-ray structure of unliganded FKBP12 and of FKBP12 in complex with FK506 and with rapamycin; these structures show localized differences in conformation and mobility in those regions of the protein that are known, by site-directed mutagenesis, to be involved in calcineurin inhibition. A comparison of 16 additional X-ray structures of FKBP12 in complex with FKBP12-binding ligands, where those structures were determined from different crystal forms with distinct packing arrangements, lends significance to the observed structural variability and suggests that it represents an intrinsic functional characteristic of the protein. Similar differences have been observed for FKBP12 before, but were considered artifacts of crystal-packing interactions. We suggest that immunosuppressive ligands express their differential effects in part by modulating the conformation of FKBP12, in agreement with mutagenesis experiments on the protein, and not simply through differences in the ligand structures themselves.

### Introduction

FK506 (Prograf®; USAN tacrolimus) is a natural product screening lead (Kino *et al.*, 1987) that acts as a down-regulatory agonist on $Ca^{2+}$-dependent activation pathways in T-cells, by interrupting transcription of interleukin-2 and other T-cell activation genes (Tocci *et al.*, 1989; Mattila *et al.*, 1990; Schreiber, 1991). This mechanism is dependent on the inhibition of calcineurin, an intracellular $Ca^{2+}$-dependent phosphatase (Klee & Cohen, 1988) by the FKBP12-FK506 complex (Liu *et al.*, 1991). FKBP12 also binds a related immunosuppressant, rapamycin (Vezina, Kudelski & Sehgal, 1975) (Rapamune®; AY22989; USAN tacrolimus), which inhibits lymphocyte-induced proliferation through a mechanism distinct from that of FK506 (Dumont, Staruch, Koprak, Melino & Sigal, 1990). The mechanism of action of immunosuppressive agents has been reviewed recently (Schreiber, 1991; Sigal & Dumont, 1992; Rosen & Schreiber, 1992; Schreiber & Crabtree, 1992; Schreiber, Albers & Brown, 1993; Liu, 1993*a*,*b*; Navia & Peattie, 1993*a*,*b*; Armistead & Harding, 1993).

Roughly half of the chemical structure of FK506 is found to be homologous in rapamycin, an observation that led to a renewal of interest in that ligand's immunosuppressive properties (Tocci *et al.*, 1989). FK506 and rapamycin can each antagonize the distinct immunosuppressive effects of the other by competing for FKBP12 through the common interaction of their 'binding domains'. The structure of the bound ligands has been characterized in detail by X-ray crystallography of the respective FKBP12–ligand complexes (Van Duyne, Standaert, Karplus, Schreiber & Clardy, 1991, 1993; Van Duyne, Standaert, Schreiber & Clardy, 1991; Rotonda, Burbaum, Chan, Marcy & Becker, 1993; Becker *et al.*, 1993). Those structural studies also showed that the non-homologous 'effector-domain' regions of the ligands protrude beyond the surface of the protein with distinct conformations that might well accommodate calcineurin binding and inhibition with FK506, but neither with rapamycin.

An elegant effector-domain model has been proposed (Schreiber, 1991; Rosen & Schreiber, 1992; Schreiber & Crabtree, 1992; Liu, 1993*a*,*b*; Schreiber *et al.*, 1993) to explain the different functional consequences of ligand binding to FKBP12 in terms of these structural features. [The FKBP12–rapamycin complex, common binding to FKBP12 notwithstanding, as well as free FK506, rapamycin, and the uncomplexed FKBP12 itself, are all ineffective as calcineurin inhibitors (Schreiber, 1991; Sigal & Dumont, 1992).] The model has enjoyed broad acceptance because it is consistent with the observed

* To whom correspondence should be addressed.




ISSN 0907-4449 

Table 1. *Solved crystal structures*

Resolution = resolution of the X-ray data. *R* factor = crystallographic residual. R.m.s. bonds and r.m.s. angles = root-mean-square deviation of bond lengths and angles from ideal values. The space group and unit-cell dimensions for each solved structure are given. R.m.s.d. = root-mean-square deviation for main-chain atoms after least-squares superposition with Nati-FK506 structure.

| Crystals | Resolution (Å) | *R* factor (%) | R.m.s. bonds (Å) | R.m.s. angles (°) | Space group | *a* (Å) | *b* (Å) | *c* (Å) | α (°) | β (°) | γ (°) | R.m.s.d. main chain (Å) |
|---|---|---|---|---|---|---|---|---|---|---|---|---|
| Native | 2.2 | 15.8 | 0.017 | 3.5 | $P4_32_12$ | 34.1 | 34.1 | 202.2 | 90 | 90 | 90 | 0.51 |
| Nati-FK506 | 1.7 | 16.2 | 0.014 | 2.9 | $P4_22_12$ | 58.1 | 58.1 | 55.7 | 90 | 90 | 90 | — |
| Nati-Rapa | 1.7 | 18.1 | 0.016 | 2.9 | $P2_12_12_1$ | 48.9 | 49.5 | 55.2 | 90 | 90 | 90 | 0.64 |
| Complex 1 | 1.7 | 18.7 | 0.014 | 2.9 | *R*3 | 41.9 | 41.9 | 41.9 | 83.9 | 83.9 | 83.9 | 0.63 |
| Complex 2 | 2.3 | 17.5 | 0.019 | 3.7 | $P2_1$ | 36.5 | 92.2 | 32.9 | 90 | 117.9 | 90 | 0.47 |
| Complex 3 | 1.5 | 18.2 | 0.017 | 2.9 | $P2_12_12_1$ | 34.9 | 40.6 | 80.6 | 90 | 90 | 90 | 0.46 |
| Complex 4 | 1.9 | 18.5 | 0.017 | 3.1 | $P2_122_1$ | 28.8 | 37.3 | 98.4 | 90 | 90 | 90 | 0.42 |
| Complex 5 | 1.8 | 18.1 | 0.015 | 3.1 | $P2_12_12_1$ | 29.7 | 52.4 | 85.1 | 90 | 90 | 90 | 0.53 |
| Complex 6 | 1.9 | 19.2 | 0.017 | 3.2 | $P2_122$ | 96.2 | 37.3 | 30.7 | 90 | 90 | 90 | 0.45 |
| Complex 7 | 2.1 | 18.2 | 0.017 | 3.4 | $P2_12_12_1$ | 32.5 | 45.3 | 67.9 | 90 | 90 | 90 | 0.39 |
| Complex 8 | 1.8 | 18.9 | 0.014 | 3.1 | $P2_12_12_1$ | 29.4 | 62.4 | 112.1 | 90 | 90 | 90 | 0.44 |
| Complex 9 | 1.9 | 18.7 | 0.013 | 3.1 | $P2_12_12_1$ | 30.6 | 59.6 | 66.7 | 90 | 90 | 90 | 0.41 |
| Complex 10 | 2.1 | 20.1 | 0.015 | 3.3 | $P2_12_12_1$ | 28.9 | 49.9 | 75.1 | 90 | 90 | 90 | 0.45 |
| Complex 11 | 1.8 | 17.8 | 0.014 | 2.9 | $P2_12_12_1$ | 94.9 | 36.4 | 33.5 | 90 | 90 | 90 | 0.43 |
| Complex 12 | 2.2 | 18.7 | 0.015 | 3.3 | $P2_12_12_1$ | 50.0 | 56.2 | 73.0 | 90 | 90 | 90 | 0.49 |
| Complex 13 | 1.8 | 18.1 | 0.013 | 2.9 | $P3_2$ | 56.2 | 56.2 | 79.8 | 90 | 90 | 120 | 0.49 |
| Complex 14 | 1.8 | 18.9 | 0.013 | 3.1 | $P2_12_12_1$ | 53.1 | 69.7 | 54.8 | 90 | 90 | 90 | 0.40 |
| Complex 15 | 2.2 | 20.9 | 0.016 | 3.4 | *P*1 | 45.0 | 42.9 | 37.3 | 90 | 101 | 108 | 0.47 |
| Complex 16 | 1.8 | 20.5 | 0.012 | 1.8 | $P2_12_12_1$ | 44.0 | 72.9 | 36.4 | 90 | 90 | 90 | 0.42 |

reciprocal antagonism of FK506 and rapamycin, because it can be extended to rationalize the reduction in calcineurin inhibitory activity that accompanies minor modifications of FK506 (Tocci *et al.*, 1989; Sigal & Dumont, 1992; Armistead & Harding, 1993; Organ *et al.*, 1993; Dumont *et al.*, 1992; Parson, Sigal & Wyvratt, 1993; Kawai *et al.*, 1993; Goulet, Rupprecht, Sinclair, Wyvratt & Parsons, 1994), and because it has had predictive value in ligand design. [Support for the model was provided, for example, by the synthesis of 506BD, a binding-domain mimic devoid of effector-domain structural elements, which proved to be an antagonist of FK506-mediated calcineurin inhibition (Bierer, Somers, Wandless, Burakoff & Schreiber, 1990; Somers, Wandless & Schreiber, 1991).]

In contrast to the pivotal role assigned to FK506 in the effector-domain model, the FKBP12 protein itself was left with the minimal function of a scaffold or 'presenter' (Schreiber, 1991) of ligands to calcineurin. This hypothesis was supported by a comparison of the structures of FKBP12 in its complexes with FK506 and with rapamycin, as determined by X-ray diffraction (Van Duyne Standaert, Karplus *et al.*, 1991; Van Duyne, Standaert, Schreiber *et al.*, 1991; Van Duyne, Standaert, Karplus, Schreiber & Clardy, 1993), and of unliganded FKBP12, as determined by solution NMR methods (Michnick, Rosen, Wandless, Karplus & Schreiber, 1991; Moore, Peattie, Fitzgibbon & Thomson, 1991; Rosen, Michnik, Karplus & Schreiber, 1991), which suggested that the structure of the protein was unaffected in its conformation and mobility by ligand binding. Differences were observed between the three structures, but these were attributed to experimental artifacts, including crystal-packing interactions (Van Duyne, Standaert, Karplus *et al.*, 1991; Van Duyne, Standaert, Schreiber *et al.*, 1991; Van Duyne *et al.*, 1993) and a paucity of NMR constraints (Michnick *et al.*, 1991; Moore *et al.*, 1991; Rosen *et al.*, 1991), in specific regions of the protein, an assumption that would be prudent in a structural comparison involving a small protein like FKBP12 on the one hand, and a mix of structure-solution methodologies on the other.

Here, we report the structure of FKBP12 in its native unliganded state and in complex with FK506, with rapamycin, and with 16 other synthetic FKBP12-binding ligands (Table 1). A comparison of these structures shows that the conformation of FKBP12 can be locally modulated (Fig. 1), with differences comparable in magnitude to the structural differences observed in mutant FKBP12–FK506 complexes that are unable to inhibit calcineurin (Itoh *et al.*, 1995). These observations reinforce the view (Aldape *et al.*, 1992) that ligand-induced changes in the structure of FKBP12 may play a role in the calcineurin inhibitory potential of the protein–ligand complex.

## Materials and methods

*Bovine thymus FKBP12 (bFKBP12) purification*

Fresh bovine thymus was trimmed and cut into approximately 2.5 $cm^3$ cubes, frozen in liquid $N_2$ and stored at 203 K for later use. 3–4 kg of frozen tissue was thawed, 1 kg at a time, in 5 volumes of cold extraction buffer (100 m*M* potassium phosphate, 0.5 m*M* EDTA, 1 m*M* β-mercaptoethanol, 0.02% $NaN_3$, 0.1 m*M* PMSF) and homogenized using a Polytron (Brinkmann PT-6000, with large scale generator). After complete homogenization, chloroform was added to a final

concentration of 2.5%(*v*/*v*) and briefly mixed using the Polytron. The homogenate was centrifuged at 12 000*g* for 50 min at 278 K. The pelleted material, containing the majority of the excess chloroform, was discarded and the supernatants were combined and adjusted to 1.7 *M* potassium phosphate by addition of a 4.0 *M* (pH 7.1) stock. The solution was centrifuged again, as above, to remove any precipitated protein, and the entire supernatant from 3–4 kg of tissue was applied (flow rate 15–20 ml $min^{-1}$, at 295 K) to a 5 × 30 cm hydrophobic interaction (HIC) column (Rainin Hydropore-HIC) which had been previously equilibrated in 1.7 *M* potassium phosphate, 1 m*M* $\beta$-mercaptoethanol, pH 7.1. After washing with two column volumes of the same buffer, the bound protein was eluted at 295 K with degassed $dH_2O$ containing 1 m*M* $\beta$-mercaptoethanol. The eluted protein was concentrated by ultrafiltration to about 150 ml, and then fractionated by size-exclusion chromatography on a Pharmacia Sephacryl S-100 HR column (10 × 110 cm) equilibrated in extraction buffer. The FKBP12-containing fractions (around 65–70% of the column volume) were pooled and then adjusted to 1.7 *M* potassium phosphate by addition of a 4.0 *M* (pH 7.1) stock. This material was loaded directly onto a second HIC column (Rainin Hydropore-HIC; 2 × 30 cm; flow rate 4 ml $min^{-1}$, at 295 K). The proteins were eluted at 4 ml $min^{-1}$ with a 3 h linear gradient into degassed $dH_2O$ containing 1 m*M* $\beta$-mercaptoethanol. The bFKBP12 peak, eluting around 1.1 *M* potassium phosphate, represented more than 90% of the protein. The final yield was typically about 10–12 mg per kg of tissue.

### *Human recombinant FKBP12 (hrFKBP12) expression and purification*

High-level expression of hrFKBP12 in *E. coli* was achieved by construction of vectors containing the complete sequence for the gene, subcloned behind a phage T7 RNA polymerase promotor vector (Studier,

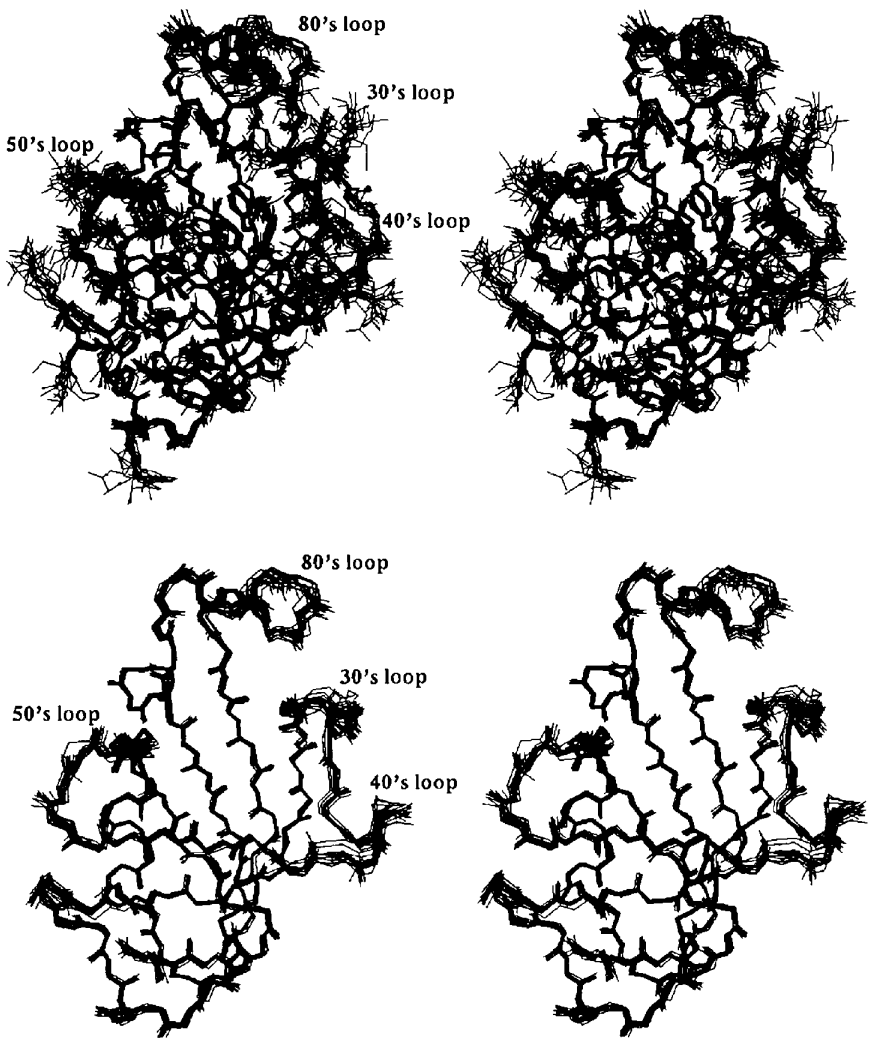


Fig. 1. Superposition of the coordinates of the 19 FKBP12 structures described in Table 1, with all main-chain and side-chain atoms shown, and with main-chain (C, N, Cα, O) atoms only. This comparison identifies regions of FKBP12 whose conformation is largely conserved (mostly localized in the framework $\beta$-sheet and $\alpha$-helix secondary structure), and other regions that show variable conformation and mobility (mostly localized in loops). The correspondence between the 19 structures shown, all from different crystal forms, suggests that experimental artifacts such as crystal contacts are not responsible for the structural differences observed, and that the rigidity of the framework and the conformational flexibility of the loops may have functional relevance.

Rosenberg, Dunn & Dubendorff, 1990). Production of hrFKBP12 was initiated by the addition of isopropyl-β-D-thiogalactopyranoside (IPTG), to a final concentration of 1 m*M*. This induces a chromosomal copy of T7 RNA polymerase (behind the *lac* UV promotor) in the host JM109/DE3, which then initiates transcription of the protein gene (Studier & Moffat, 1986). The yield from a typical culture in a 10 l fermentor (Biostat ED, B. Braun) was about 250 g of wet cell paste. The cell paste was stored frozen at 203 K prior to protein purification. Full details of the hrFKBP12 expression will be presented elsewhere. (Chambers *et al.*, unpublished work)

Typically, about 500 g of frozen cell paste was thawed and slurried in four additional volumes of cold buffer [50 m*M* potassium phosphate, 1 m*M* EDTA, 1 m*M* β-mercaptoethanol and 0.1 m*M* phenylmethylsulfonylfluoride, pH (278 K) = 7.0]. The slurry was briefly homogenized by mechanical disruption in a Polytron blender, as above, and then the cells were fully lysed by three serial passages through a high-pressure laboratory homogenizer (Rannie, Mini-lab 8.30H) at 9000 psi. After each passage, the lysed cell suspension was collected on ice, and afterwards centrifuged at 12 000*g* for 50 min at 278 K. The clarified extract was passed through a 5 × 30 cm column of Pharmacia Fast Flow DEAE Sepharose (equilibrated at 278 K in the cell-extraction buffer), and the column flow-through and wash were collected. This was concentrated by ultrafiltration and subjected to size-exclusion and hydrophobic interaction chromatography essentially as described for the bovine thymus protein. From the 500 g of cell paste, about 3.5 g of hrFKBP12 was obtained.

*Protein characterization*

Both bFKBP12 and hrFKBP12 were judged better than 99% pure by sodium dodecyl sulfate polyacrylamide gel electrophoresis and reversed phase high pressure liquid chromatography. Purity and enzymatic integrity were further confirmed by N-terminal sequence analysis, by analysis of ($^3$H)dihydro-FK506 binding activity (essentially as described by Park, Aldape, Futer, DeCenzo & Livingston, 1992), and by enzymatic analysis of the peptidyl-prolyl isomerase activity (essentially as described by Harrison & Stein, 1990). The specific peptidyl–prolyl isomerase and tacrolimus binding activities of both proteins were equal to or greater than those previously reported (Siekierka, Hung, Poe, Lin & Sigal, 1989; Harding, Galat, Uehling & Schreiber, 1989; Park *et al.*, 1992), and all of the peptidyl–prolyl *cis–trans* isomerase activity of each protein was inhibitable by FK506 and was unaffected by cyclosporin A. All buffer-exchange and protein concentration steps were carried out by ultrafiltration, in a stirred cell (5000 $M_r$ cut-off membrane) under $N_2$ pressure at 278 K. The protein was stored in 10 m*M* sodium cacodylate (pH 6.5), at 203 K until needed. All protein concentrations were

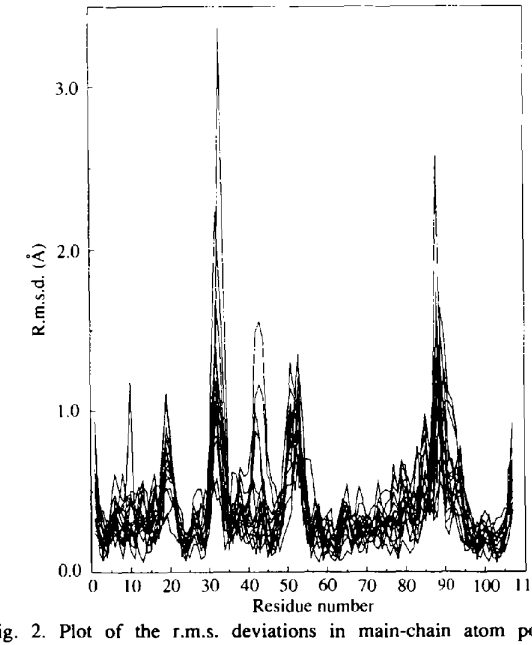


Fig. 2. Plot of the r.m.s. deviations in main-chain atom positions of the structures included in Table 1 after superposition onto the hrFKBP12–FK506 complex structure. The conformational flexibility in the loop regions is once again evident.

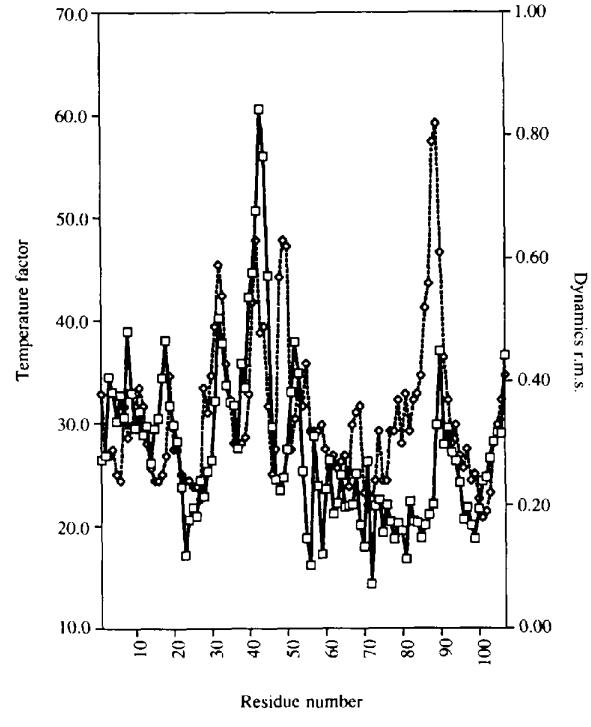


Fig. 3. Plot of the temperature factors (Å$^2$) of the Cα atoms of the structure of the unliganded bFKBP12 superimposed on the r.m.s. deviation motion of the Cα atoms from the 100 ps dynamics runs on solvated unliganded bFKBP12.

determined using a molar absorption coefficient ($A_{280}$) of 9600 $M^{-1}$ cm$^{-1}$

*Preparation of FKBP12–drug complexes*

Protein–drug complexes were prepared by addition of a drug stock solution (ligand at 20 mg ml$^{-1}$ in dimethyl sulfoxide) to 1 mg ml$^{-1}$ solutions of FKBP12 to achieve a protein:drug molar ratio of from 1:1.25 to 1:1.5. The protein complexes were then concentrated by ultrafiltration and washed with fresh 10 m*M* sodium cacodylate (pH 6.5) until the dimethyl sulfoxide concentration was less than 0.001%(*v*/*v*). The protein complexes were concentrated to 15–150 mg ml$^{-1}$, depending on the observed solubility of each complex. Samples were finally centrifuged at 278 K for 20–30 min at about 30 000*g* to remove microscopic debris, and stored at 253 K until crystallization trials began.

*Structure determination of unliganded bFKBP12*

Crystals of unliganded bFKBP12 were grown both in the laboratory and in a microgravity environment on board the United States Microgravity Laboratory-1 (USML-1) during mission STS-50 of the space shuttle orbiter Columbia, as described (DeLucas *et al.*, 1994). The crystallization conditions used were developed and optimized for earth-bound crystals. In both situations, tetragonal crystals of bFKBP12 ($P4_32_12$; $a$ = 34.38, $c$ = 202.01 Å) were grown at room temperature from 140 mg ml$^{-1}$ protein solutions by vapor diffusion against 1.4–1.6 *M* sodium sulfate in 100 m*M* cacodylate buffer at pH 7.5; macroseeding was required for diffraction-quality crystals. On the whole, crystals of unliganded bFKBP12 diffract poorly when compared to crystals of FKBP12 complexes (Table 1). Crystal growth in microgravity significantly improved the signal-to-noise ratio and resolution of the diffraction data obtained, however, as described previously (DeLucas *et al.*, 1994). All data were collected on an R-AXIS II area detector (Rigaku/MSC, Woodland, TX). 10 574 reflections (3977 unique) were measured from a single crystal obtained from the microgravity experiment, to 2.3 Å resolution (68% of total available), with a symmetry $R$ factor for the data of 4.9% on intensities. Initial phase information was obtained by Patterson correlation molecular replacement (Brünger, 1990*a*) using coordinates from an earlier structure determination of the FKBP12–FK506 complex (Van Duyne, Standaert, Karplus *et al.*, 1991); Protein Data Bank accession number 1FKF (Bernstein *et al.*, 1977). Alternating cycles of map interpretation using the program *QUANTA* (Version 3.3; Molecular Simulations Inc., 1993) and of simulated annealing with *X-PLOR* (Brünger, 1990*b*; Brünger, Krukowski & Erickson, 1990) were used to refine the model, with 67 water molecules built into difference electron density. Final refinement reduced the $R$ factor to 15.8% at 2.3 Å resolution with reasonable geometry [deviation from ideality was 0.017 Å for bond lengths, 3.45° for bond angles and 1.90° for improper dihedrals; see Brünger (1990*b*) for definitions]. In contrast, an equivalent level of refinement ($R$ factor = 15.9%) with similar geometry was only achievable at 3.1 Å resolution with unit-gravity data.

*Structure of the bFKBP12–rapamycin complex*

A 10 mg ml$^{-1}$ solution of bFKBP12 in complex with rapamycin was crystallized by vapor diffusion against 50 m*M* ammonium sulfate and 200 m*M* potassium phosphate at pH 5.5, the space group is $P2_12_12_1$ with cell dimensions $a$ = 45.86, $b$ = 49.46, $c$ = 55.20 Å. Crystals were similar to those reported earlier for the hrFKBP12–rapamycin complex (Van Duyne, Standaert, Schreiber *et al.*, 1991), even though bFKBP12 was used here instead. The crystal structure was solved

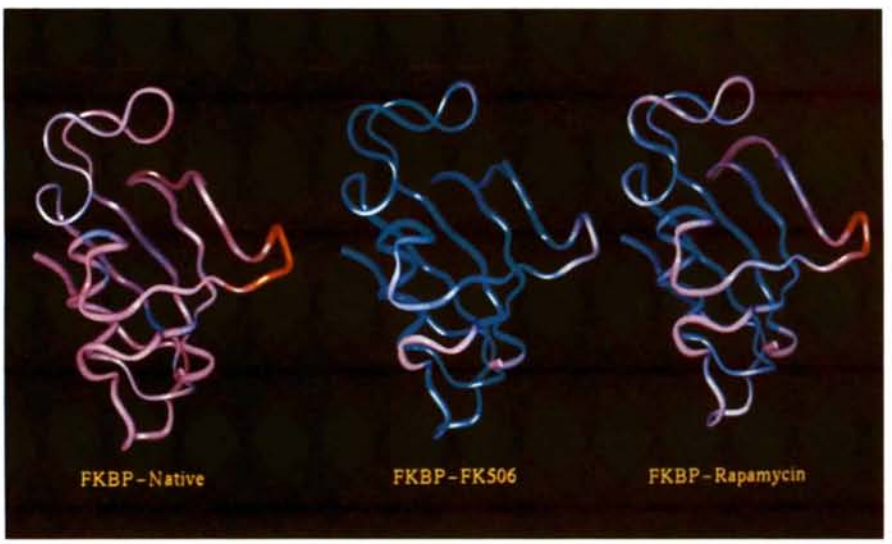


Fig. 4. Schematic comparison of the structures of unliganded bFKBP12, hrFKBP12 in complex with FK506, and bFKBP12 in complex with rapamycin. Structures are color coded by temperature factor; lowest in blue and highest in red. These data suggest that FK506 binding to FKBP12, which leads to a productive inhibition of calcineurin activity, may considerably restrict the overall mobility of FKBP12, in agreement with molecular-dynamics simulations.

by molecular replacement using coordinates from the hrFKBP12–FK506 complex structure described below. 11 083 unique reflections were observed to 1.77 Å resolution (90% of the total available). Refinement led to an $R$ factor for the final model of 17.7%. Deviation from ideality was 0.016 Å for bond lengths, 2.94° for bond angles and 1.24° for improper dihedrals. The final atomic model consisted of 889 heavy protein atoms and 102 water molecules.

*Structure of the hrFKBP12–FK506 complex*

Crystals of the hrFKBP12–FK506 complex were obtained as described previously (Van Duyne, Standaert, Karplus *et al.* 1991), except that the crystallization was carried out at pH 7.0 instead of pH 5.6. Crystals were grown by vapor diffusion from a 20 mg ml$^{-1}$ solution of hrFKBP12 in complex with FK506, against a reservoir of 1.7 $M$ ammonium sulfate in 200 m$M$ cacodylate at pH 7.0; the space group is $P4_22_12$ with cell dimensions $a$ = 58.07, $c$ = 55.65 Å. Data were collected and processed as above. 8743 unique reflections were observed to 1.76 Å resolution (90% of those available). Refinement was as described above, with starting coordinates taken from the earlier determination of the hrFKBP12–FK506 complex (Van Duyne, Standaert, Karplus *et al.*, 1991). Refinement led to a final $R$ factor of 16.2% with good geometry (deviation from ideality was 0.014 Å for bond lengths, 2.87° for bond angles, and 1.15° for improper dihedrals). No significant differences were noted between the reported hrFKBP12–FK506 complex structure at pH 5.6 (Van Duyne, Standaert, Karplus *et al.*, 1991) and our structure at pH 7.0. The final atomic model consisted of 889 heavy protein atoms and 97 water molecules.

*Structure comparisons*

Structures of the unliganded FKBP12 and of the FKBP12 complexes with FK506 and with rapamycin were superimposed by a least-squares procedure within *X-PLOR* (Brünger, 1990*b*) that overlapped all main-chain atoms (C, N, O, Cα) of the protein. Calculated r.m.s. positional differences between the structures were 0.51 Å for the unliganded bFKBP12 *versus* the hrFKBP12–FK506 complex, 0.64 Å for bFKBP12 *versus* the bFKBP12–rapamycin complex, and 0.67 Å for the hrFKBP12–FK506 *versus* the bFKBP12–rapamycin complexes. Crystallization, structure determination and refinement parameters for these structures, and the 16 other inhibitor complex structures under discussion are summarized in Table 1.

*Molecular-dynamics simulations*

Molecular-dynamics simulations used the program *CHARMm* (Version 2.2) (Brooks *et al.*, 1983), as implemented within *QUANTA* (Version 3.3, Molecular Simulations Inc., 1993). Starting bFKBP12 coordinates were taken from this study. A subset of approximately ten crystallographically determined bound waters were included in the simulation, where the choice of these was based on thermal-factor data and visual examination of coordinates and maps. H atoms were added with *CHARMm*, and the resulting structures were energy minimized to a gradient of 0.04184 kJ Å$^{-2}$ (0.01 kcal Å$^{-2}$). For these simulations, a distant-dependent dielectric ($\varepsilon = r$) was used. Molecular dynamics were initiated by heating the structures from 0 K to 300 K during 5 ps, and then allowing the systems to equilibrate at 300 K for 25 ps. At that point, data accumulation was begun,

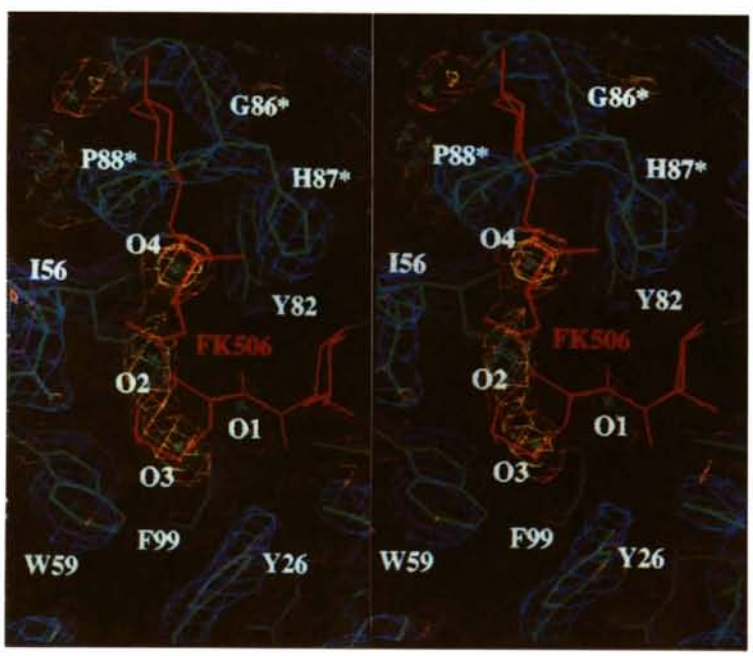


Fig. 5. Electron-density map of the ligand-binding cavity of unliganded bFKBP12, calculated with $2|F_o| - |F_c|$ 2.0 standard deviation units above background (blue), and with $|F_o| - |F_c|$ coefficients, contoured at 2.0 (yellow) and 3.0 (orange) standard deviation units above background. Superimposed on the density are the coordinates of the unliganded bFKBP12 (green) and of the hrFKBP12 complex with FK506 (violet). The excellent overall fit of these coordinates is indicative of how similar are the conformations adopted by the three FKBP12's are in this region of the protein (for clarity, the rapamycin complex coordinates are not shown). Note that binding of FK506 (and of rapamycin) rotates the side chain of Trp59 when compared to the unliganded structure. The perturbation of Trp59 upon ligand binding may be responsible for the fluorescence changes previously reported on binding (Park *et al.*, 1992).

and continued for an additional 100 ps at 300 K with trajectories saved every 0.5 ps (for a total of 201 coordinate sets for each system). To test the stability of our model, native FKBP12 was subjected to an additional 200 ps of simulation, with trajectories saved every 0.5 ps. As a control, a fully solvated run was carried out on the native enzyme using a constant dielectric ($\varepsilon$ = 1). Approximately 200 water molecules were placed in the active site and a weak restraining force was used to prevent solvent drift. A non-bond cutoff of 12 Å was used for all simulations.

## Results

### *Comparison of the structure of liganded and unliganded FKBP12's*

In order to explore the possible mechanistic role of subtle conformational variability in FKBP12, we have solved the structures of unliganded bovine bFKBP12 (at 2.3 Å resolution, $R$ = 15.8%) and of bFKBP12 in complex with rapamycin (1.77 Å resolution, $R$ = 17.7%). Both are reported here for the first time. We have also re-determined independently the structure of the hrFKBP12 complex with FK506 (1.76 Å resolution, $R$ = 16.2%). Our analysis of protein conformation and mobility has been extended to include 16 other FKBP12 complex structures from our immunosuppressant drug design program (unpublished data), where these have been solved in different crystal forms with distinct packing arrangements and crystal contacts. These structures are summarized in Table 1, which lists space group, unit cell, data collection and refinement parameters. The ligands used were typically tight-binding linear diketo pipecolate analogs, including the compound whose complex structure is described in the accompanying paper (Armistead *et al.*, 1995); none of these ligands is able to inhibit calcineurin in complex with FKBP12, however.

All 19 FKBP12 structures are superimposed in Fig. 1, which contrasts the close alignment found in the framework regions of the molecule with the mobility of the loops. Taken together with the r.m.s. deviation of main-chain atoms calculated for the 19 superimposed structures (Fig. 2), these data suggest that the observed variability in FKBP12 is intrinsic to the protein, and that FKBP12 is subject to significant localized changes in conformation and mobility as a consequence of ligand binding. Support for this view is derived from an analysis of molecular-dynamics simulations and from generalized order parameter data obtained by $^{1}H$-$^{15}N$ NMR spectroscopy (Cheng *et al.*, 1993).

### *Molecular-dynamics simulations*

Fig. 3 shows that there is general agreement between the r.m.s. deviation of Cα-atom positions taken from the 300 ps molecular-dynamics simulation of solvated unliganded FKBP12, and the scaled Cα-atom temperature factors taken from the corresponding unliganded bFKBP12 structure. The molecular-dynamics simulation suggests that the '80's loop' (Fig. 1) delimited by Thr85 and Asn94 may move cooperatively, as a flap (see Fig. 3), with the variability for the $\varphi$–$\psi$ angles of the residues at the ends of the loop suggesting a hinge. The overall mobility of the 80's loop can be monitored by the average distance from the Cα atom of Trp59 at the base of the ligand-binding site to that of His87 at the tip of the 80's loop. In the unliganded FKBP12 simulation, the average distance is 18.2 Å with an r.m.s. deviation of ±1.7 Å. For the FK506 complex, however, the average distance decreases to 16.7 Å and the r.m.s. deviation is only 0.8 Å. This restriction in flap mobility is apparently due to favorable van der Waals interactions between the pyran ring and its substituents on FK506 with residues His87 and Ile91 on the protein. Dynamics simulation of the FKBP12–rapamycin complex shows that the average distance and r.m.s. deviation between Trp59 and His87 is only slightly reduced when compared to the unliganded protein. Rapamycin has a different substitution pattern on the pyran ring and consequently makes fewer van der Waals interactions. This pattern of restricted mobility suggests that the structure of FKBP12 in complex with FK506 is significantly more ordered than either the rapamycin complex or the unliganded protein, in agreement with corresponding X-ray temperature-factor data (Fig. 4). NMR dynamics studies of free and FK506-bound FKBP12 (Cheng *et al.*, 1993) also show that the 80's loop becomes fixed on binding ligand.

### *Solvent structure in the active site*

Few ordered water molecules are found in the generally hydrophobic environment of the binding cavity of unliganded FKBP12 (Fig. 5). Nonetheless, these solvent molecules appear to be important contributors to the binding of FKBP12 ligands and substrates. A comparative thermodynamic and structural study of wild-type and mutant (Tyr82Phe) hrFKBP12's in complex with FK506 (Connelly *et al.*, 1993) concluded that the expulsion of two of these water molecules made a favorable entropic contribution to the overall binding of FK506.

The C8 carbonyl O atom of FK506 (nomenclature as defined in the accompanying paper, Armistead *et al.*, 1995) is thought to resemble the *trans*-prolyl carbonyl of a peptide substrate; the C9 carbonyl O atom is thought to mimic the twisted amide transition state for the PPIase activity of FKBP12 (Schreiber, 1991; Rosen & Schreiber, 1992; Rosen, Standaert, Galat, Nakatsuka & Schreiber, 1990). In the structure of the complex with FKBP12, the C8 carbonyl O atom of FK506 forms a good hydrogen bond with Tyr82 OH (2.8 Å), while the C9 carbonyl O atom interacts with the edges of Phe36 (3.4 Å to CZ), Tyr26 (3.5 Å to CE1) and Phe99 (3.6 Å to CE1) (Van Duyne, Standaert, Karplus *et al.*,

1991; Van Duyne *et al.*, 1993; and this work). The electron density corresponding to water molecule O1 is centered 3.3 Å from Tyr82 OH, and 3.4 and 3.8 Å from CE2 and CZ of Phe36 and Phe99, respectively (Fig. 5). The temperature factor for O1 is high (55.8 $Å^2$), however, with diffuse density suggestive of multiple solvent sites, each of which may satisfy the interactions observed for FK506. Water molecule O2 occupies a small hydrophobic/aromatic cavity composed of Val55, Ile56, Phe46 and Trp59 with strong electron density, and is directly hydrogen bonded to the amide N atom of Ile56; O2 corresponds most closely to the C1 carbonyl O atom of FK506. Connected density to water molecules O3 and O4 is evident in this region when one contours at a lower level, however. This density partially overlaps the space occupied by bound FK506, which acts as a twisted amide peptide analog, and may be suggestive of a partially occupied dipeptide in the active site.

We also observe a distinct difference in the orientation of the side chain of Trp59 in the unliganded state when compared to that observed on binding of either FK506 (Fig. 5) or rapamycin (similar data not shown). The perturbation of Trp59 upon ligand binding may be responsible for the fluorescence changes previously reported (Park *et al.*, 1992).

*Comparison of sequence and structural data*

FKBP12 sequences across species as distant as mammals and fungi are strongly conserved, more so than the sequences of other FK506 binding proteins (FKBP's) within a species (Peattie *et al.*, 1992, and references therein). This is not surprising for those residues that are directly involved in ligand binding. However, many conserved residues are found on the distal side of the $\beta$-sheet framework of the molecule, well away from the binding cavity for immunosuppressant ligands and the prolyl isomerase active site. Some of these residues are clearly involved in hydrophobic and salt-bridge interactions that may serve to stabilize the protein, but some have no obvious reason to explain their conservation, and may well be involved in as yet undiscovered interactions.

Synthesis of FK506 by its producing organism may confer a competitive advantage upon it, by inhibiting the FKBP12's of competing microbial species. As fungal metabolites (Kino *et al.*, 1987; Vezina *et al.*, 1975), however, neither FK506 nor rapamycin are likely themselves to be the endogenous ligand(s) that normally interact with the mammalian FKBP12's; nor is there currently any direct evidence for the existence of such. By looking at the pattern of contiguous conserved residues in the structure of FKBP12, however, one can discern what might be the 'footprint' of such an endogenous ligand (Fig. 6), in the form of a continuous slot extending beyond the FK506-binding site. The slot is largely hidden by residues of the 80's loop, but these have been shown to behave as a mobile flap in the molecular-dynamics simulations described above. As with the aspartyl proteases (Davies, 1990; Wlodawer & Erickson, 1993) and various lipases (Cambillau & van Tilbeurgh, 1993), conserved structural elements protected by a flap hint at functionality (Sali *et al.*, 1992), and one can speculate on the possible displacement of the flap as a component of the binding of the unknown endogenous ligand, or of calcineurin. Site-directed mutagenesis of the conserved residues of the footprint region may clarify their role in the function of FKBP12.

## Discussion

The differences in FKBP12 structure that we have described suggest that the conformation of the protein may be important in establishing the calcineurin inhibitory potential of a given ligand complex, and that immunosuppressive ligands like FK506 may express

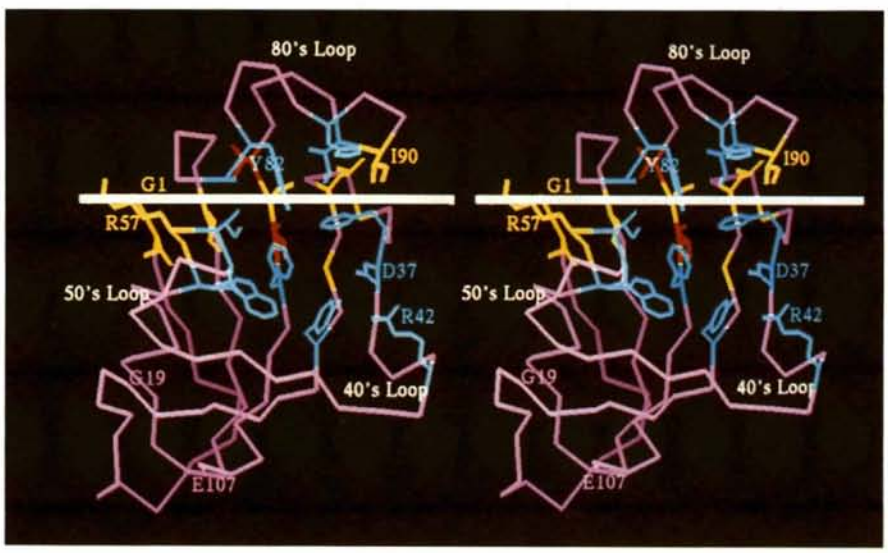


Fig. 6. C$\alpha$ trace of the structure of unliganded bFKBP12 shown in stereo. Conserved residues associated with FK506 binding are shown in blue; conserved residues contiguous to the latter are in yellow; contiguous backbone atoms are in orange. The combined pattern of conserved residues is suggestive of a 'footprint' of interaction for the putative endogenous FMBP12 ligand that FK506 may mimic. The footprint of conserved residues on the surface of FKBP12 forms a slot that extends away from the FK506 binding cavity to the surface of the protein. The slot is protected by residues Thr85 to Asp94, which molecular-dynamics simulations suggest may be mobile as a unit, acting as a 'flap', such as is found, for example, in HIV-1 protease and other members of the aspartyl protease family (see text).

their differential effects in part by modulating the protein conformation. This point is illustrated by the breakdown of the effector-domain model in explaining the remarkable behavior of L-658,818 (a close 18-hydroxyl-21-ethyl analog of FK506) (Rotonda *et al.*, 1993; Becker *et al.*, 1993; Parson *et al.*, 1993). In complex with hrFKBP12, L-658,818 acts as an antagonist of calcineurin inhibition, much like rapamycin; in complex with yeast FKBP12, however, L-658,818 becomes a more potent inhibitor of calcineurin phosphatase activity than FK506 itself (Rotonda *et al.*, 1993; Parson *et al.*, 1993). The Merck group has compared the structures of FK506* in complex with human and yeast FKBP12's, respectively, and has found, in addition to the obvious side-chain substituents, main-chain r.m.s. differences corresponding to those found in the regions of mobility identified in this study (Figs. 1–4). Least affected by its binding to the human and yeast FKBP12's was the conformation of FK506 itself, with an r.m.s. deviation between structures of only 0.35 Å (Rotonda *et al.*, 1993), a figure that is roughly comparable to the expected error of the method (Rotonda *et al.*, 1993; Becker *et al.*, 1993).

The structures of mutant FKBP12's in complex with FK506 (Itoh *et al.*, 1995; Lepre *et al.*, unpublished work), along with the limited functional data available for FK506 analogs (Tocci *et al.*, 1989; Sigal & Dumont, 1992; Armistead & Harding, 1993; Organ *et al.*, 1993; Dumont *et al.*, 1992; Parson *et al.*, 1993; Kawai *et al.*, 1993; Goulet *et al.*, 1994), all support the existence and importance of a composite surface of ligand and protein structural elements whose integrity is critical for calcineurin inhibition (Aldape *et al.*, 1992). Within this interaction region (Fig. 7), we have identified several prominent depressions on the surface of the FKBP12–FK506 complex that are either distorted or blocked outright in antagonist complexes. Significantly, the constituent amino acids that form a part of these composite depressions are those whose mutation most severely affects calcineurin inhibition by the corresponding FKBP12–FK506 complex, and whose location can also be mapped to the regions of FKBP12 conformational variability that we have identified (Figs. 1–4) in this study.

## Concluding remarks

The foundations of the effector-domain model depend on a correlation between the agonist and antagonist behavior of FK506 and rapamycin in promoting calcineurin inhibition (Schreiber, 1991; Rosen & Schreiber, 1992; Schreiber & Crabtree, 1992; Liu, 1993*a*,*b*; Schreiber *et al.*, 1993), and the differences in structure between the two ligands in their respective FKBP12 complexes (Van Duyne, Standaert, Karplus *et al.*, 1991; Van Duyne, Standaert, Schreiber *et al.*, 1991; Van Duyne *et al.*, 1993). If one is to generalize the model beyond those defining examples and specifically, if one is to attribute a special role to the particular FK506 effector-domain conformation that is seen in its FKBP12 complex, then it becomes necessary to assume that the protein remains 'nearly identical' (Schreiber *et al.*, 1993) in the various possible ligand bound and unbound states, and hence functionally irrelevant to any of them. These assumptions have been particularly attractive with respect to structure-based drug design in this area, since they justify simple mimicry of the FK506 effector-domain conformation as a target strategy (see, *e.g.*, the accompanying paper, Armistead *et al.*, 1995, and references therein).

Our results suggest that the interactions involved in calcineurin inhibition by FKBP12–ligand complexes are more complicated than previously recognized, and

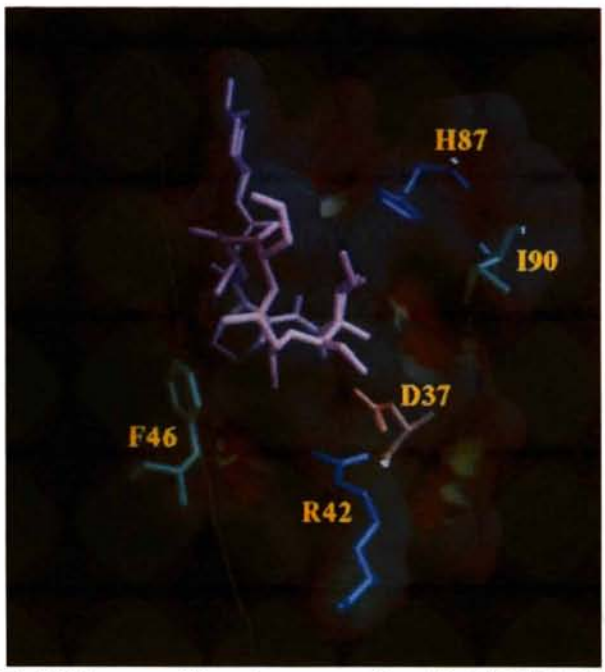


Fig. 7. Solvent-accessible surface representation of the FKBP12–FK506 complex structure. The surface is color coded with respect to its curvature, from concave (in red) to convex (in blue), as calculated by the program *GRASP* (Nicholls & Honig, 1992). Side chains for those residues known to be involved in calcineurin inhibition by site-directed mutagenesis studies (Aldape *et al.*, 1992; Yang, Rosen & Schreiber, 1993) are also displayed. A number of suggestive depressions are found in the functionally important region of the complex surrounding the bound ligand, including the 'catcher's mitt' (see text) formed by FK506 and protein residues Asp37, His87 and Ile90. A second depression involves residues Arg42 and Phe46. Ligand-induced conformational changes, or mutations (Aldape *et al.*, 1992; Itoh *et al.*, 1995) in this mobile region of the protein could alter the conformation of these surface depressions (or could eliminate them altogether), thereby preventing the binding and inhibition of calcineurin.

* The conformation of L-685,818 strongly resembles that of FK506 in its complex with human recombinant FKBP12 (r.m.s. $\Delta$ for all atoms = 0.35 Å, Becker *et al.*, 1993). As such, it was reasonably assumed that L-685,818 would adopt the same conformation found for FK506 in the yeast complex (Rotonda *et al.*, 1993). The structure of yeast FKBP12 in complex with L-685,818 has not been reported, however.

that local conformational flexibility may be an intrinsic characteristic of FKBP12 that has functional implications. In this context, the observed antagonism of the synthetic effector-less ligand 506BD (Bierer *et al.*, 1990; Somers *et al.*, 1991), though critical in gaining acceptance for the model, fails to support the proposed sufficiency of the effector-domain in promoting agonist calcineurin inhibitory activity. In addition, the structural and biochemical consequences on calcineurin inhibition of FK506 analogs like L-688,518 in complex with FKBP12 (Rotonda *et al.*, 1993; Becker *et al.*, 1993; Parson *et al.*, 1993), and of FK506 itself in complex with site-directed mutants of FKBP12, are consistent with a critical role for the FKBP12 protein, but are difficult to reconcile with the effector-domain hypothesis as it stands.

Success in the design of novel immunosuppressants that operate through the calcineurin pathway may have to take specific account of the participation of the FKBP12 protein in the interaction with calcineurin, and may ultimately require that we reconsider the design process as an enzyme inhibitor problem in the context of a solved structure of the FKBP12–FK506 complex bound to calcineurin itself.

We would like to thank our colleagues for their continuing support, and especially Stephen Chambers, David Armistead, Michael Badia, John Duffy, Jeff Saunders, David Livingston, Steve Park and Vicki Sato.

### References


ALDAPE, R. A., FUTER, O., DECENZO, M. T., JARRETT, B. P., MURCKO, M. A. & LIVINGSTON, D. J. (1992). *J. Biol. Chem.* **267**, 16029–16032.

ARMISTEAD, D. M., BADIA, M. C., DEININGER, D. D., DUFFY, J. P., SAUNDERS, J. O., TUNG, R. D., THOMSON, J. A., DECENZO, M. T., FUTER, O., LIVINGSTON, D. J., MURCKO, M. A., YAMASHITA, M. M. & NAVIA, M. A. (1995). *Acta Cryst.* D**51**, 522–528.

ARMISTEAD, D. M. & HARDING, M. W. (1993). *Annu. Rep. Med. Chem.* **28**, 207–215.

BECKER, J. W., ROTONDA, J., MCKEEVER, B. M., CHAN, H. K., MARCY, A. I., WIEDERRECHT, G., HERMES, J. D. & SPRINGER, J. P. (1993). *J. Biol. Chem.* **268**, 11335–11339.

BERNSTEIN, F. C., KOETZLE, T. F., WILLIAMS, G. J. G., MEYER, E. F. JR, BRICE, M. D., RODGERS, J. R., KENNARD, O., SHIMANOUCHI, T. & TASUMI, M. (1977). *J. Mol. Biol.* **112**, 535–542.

BIERER, B. E., SOMERS, P. K., WANDLESS, T. J., BURAKOFF, S. J. & SCHREIBER, S. L. (1990). *Science*, **250**, 556–559.

BROOKS, B. R., BRUCCOLERI, R. E., OLAFSON, B. D., STATES, D. J., SWAMINATHAN, S. & KARPLUS, M. (1983). *J. Comput. Chem.* **4**, 187–217.

BRÜNGER, A. T. (1990*a*). *Acta Cryst.* A**46**, 46–57.

BRÜNGER, A. T. (1990*b*). *X-PLOR Manual, Version* 2.1, Yale Univ., New Haven, CT, USA.

BRÜNGER, A. T., KRUKOWSKI, A. & ERICKSON, J. (1990). *Acta Cryst.* A**46**, 585–593.

CAMBILLAU, C. & VAN TILBEURGH (1993). *Curr. Op. Struct. Biol.* **3**, 885–895.

CHENG, J.-W., LEPRE, C. A., CHAMBERS, S. P., FULGHUM, J. R., THOMSON, J. A. & MOORE, J. M. (1993). *Biochemistry*, **32**, 9000–9010.

CONNELLY, P. R., ALDAPE, R. A., BRUZZESE, F. J., CHAMBERS, S. P., FITZGIBBON, M. J., FLEMING, M. A., ITOH, S., LIVINGSTON, D. J., NAVIA, M. A., THOMSON, J. A. & WILSON, K. P. (1993). *Proc. Natl Acad. Sci USA*, **91**, 1964–1968.

DAVIES, D. R. (1990). *Annu. Rev. Biophys. Biophys. Chem.* **19**, 189–215.

DELUCAS, L. J., LONG, M. M., MOORE, K. M., ROSENBLUM, W. M., BRAY, T. L., SMITH, C., CARSON, M., NARAYANA, S. V. L., HARRINGTON, M. D., CARTER, D., CLARK, A. D., JR, NANNI, R. G., DING, J., JACOBO-MOLINA, A., KAMER, G., HUGHES, S. H., ARNOLD, E., EINSPAHR, H. M., CLANCY, L. L., RAO, G. S. J., COOK, P. F., HARRIS, B. G., MUNSON, S. H., FINZEL, B. C., MCPHERSON, A., WEBER, P. C., LEWANDOWSKI, F. A., NAGABHUSHAN, T. L., TROTTA, P. P., REICHERT, P., NAVIA, M. A., WILSON, K. P., THOMSON, J. A., RICHARDS, R. N., BOWERSOX, K. D., MEADE, C. J., BAKER, E. S., BISHOP, S. P., DUNBAR, B. J., TRINH, E., PRAHL, J., SACCO, A. & BUGG, C. E. (1994). *J. Cryst. Growth*, **135**, 183–195.

DUMONT, F. J., STARUCH, M. J., KOPRAK, S. L., MELINO, M. R. & SIGAL, N. H. (1990). *J. Immunol.* **144**, 251–258.

DUMONT, F. J., STARUCH, M. J., KOPRAK, S. L., SIEKIERKA, J. J., LIN, C. S., HARRISON, R., SEWELL, T., KINDT, V. M., BEATTIE, T. R., WYVRATT, M. & SIGAL, N. H. (1992). *J. Exp. Med.* **176**, 751–760.

GOULET, M. T., RUPPRECHT, K. M., SINCLAIR, P. J., WYVRATT, M. J. & PARSONS, W. H. (1994). *Persp. Drug Disc. Design*, **2**, 145–162.

HARDING, M. W., GALAT, A., UEHLING, D. E. & SCHREIBER, S. L. (1989). *Nature (London)*, **341**, 758–760.

HARRISON, R. K. & STEIN, R. L. (1990). *Biochemistry*, **29**, 3813–3816.

ITOH, S., DECENZO, M. T., ALDAPE, R. A., LIVINGSTON, D. J., PEARLMAN, D. A. & NAVIA, M. A. (1995). Submitted.

KAWAI, M., LANE, B. C., HSIEH, G. C., MOLLISON, K. W., CARTER, G. W. & LULY, J. R. (1993). *FEBS Lett.* **316**, 107–113.

KINO, T., HATANAKA, H., HASHIMOTO, M., NISHIYAMA, M., GOTO, T., OKUHARA, M., KOHSAKA, M., AOKI, H. & IMANAKA, H. (1987). *J. Antibiot. (Tokyo)*, **40**, 1249–1255.

KLEE, C. B. & COHEN, P. (1988). *Mol. Aspects Cell. Regul.* **5**, 225–248.

LIU, J. (1993*a*). *Trends Pharmacol. Sci.* **14**, 182–188.

LIU, J. (1993*b*). *Immunol. Today*, **14**, 290–295.

LIU, J., FARMER, J. D., LANE, W. S., FRIEDMAN, J., WEISSMAN, I. & SCHREIBER, S. L. (1991). *Cell*, **66**, 807–815.

MATTILA, P. S., ULLMAN, K. S., FIERING, S., EMMEL, E. A., MCCUTCHEON, M., CRABTREE, G. R. & HERZENBERG, L. A. (1990). *EMBO J.* **9**, 4425–4432.

MICHNICK, S. W., ROSEN, M. K., WANDLESS, T. J., KARPLUS, M. & SCHREIBER, S. L. (1991). *Science*, **252**, 836–839.

Molecular Simulations Inc. (1993). *QUANTA*. Version 3.3, Molecular Simulations Inc., Burlington, MA, USA.

MOORE, J. M., PEATTIE, D. A., FITZGIBBON, M. J. & THOMSON, J. A. (1991). *Nature (London)*, **351**, 248–250.

NAVIA, M. A. & PEATTIE, D. A. (1993*a*). *Trends Pharmacol. Sci.* **14**, 189–195.

NAVIA, M. A. & PEATTIE, D. A. (1993*b*). *Immunol. Today*, **14**, 296–302.

NICHOLLS, A., & HONIG, B. (1992). *GRASP: Graphical Representation and Ananlysis of Surface Properties*, Columbia Univ., New York, USA.

ORGAN, H. M., HOLMES, M. A., PISANO, J. M., STARUCH, M. J., WYVRATT, M. J., DUMONT, F. J. & SINCLAIR, P. J. (1993). *Bioorg. Med. Chem. Lett.* **3**, 657–662.

PARK, S. T., ALDAPE, R. A., FUTER, O., DECENZO, M. T. & LIVINGSTON, D. J. (1992). *J. Biol. Chem.* **267**, 3316–3324.

PARSON, W. H., SIGAL, N. H. & WYVRATT, M. J. (1993). *Ann. NY Acad. Sci.* **685**, 22–36.

PEATTIE, D. A., HARDING, M. W., FLEMING, M. A., DECENZO, M. T., LIPPKE, J. A., LIVINGSTON, D. J. & BENASUTTI, M. (1992). *Proc. Natl Acad. Sci. USA*, **89**, 10974–10978.

ROSEN, M. K., MICHNIK, S. W., KARPLUS, M. & SCHREIBER, S. L. (1991). *Biochemistry*, **30**, 4774–4789.

ROSEN, M. K. & SCHREIBER, S. L. (1992). *Angew. Chem. Intl. Ed. Engl.* **31**, 384–400.

ROSEN, M. K., STANDAERT, R. F., GALAT, A., NAKATSUKA, M. & SCHREIBER, S. L. (1990). *Science*, **248**, 863–866.

ROTONDA, J., BURBAUM, J. J., CHAN, K. H., MARCY, A. I. & BECKER, J. W. (1993). *J. Biol. Chem.* **268**, 7607–7609.

SALI, A., VEERAPANDIAN, B., COOPER, J. B., MOSS, D. S., HOFMANN, T. & BLUNDELL, T. L. (1992). *Proteins*, **12**, 158–170.

SCHREIBER, S. L. (1991). *Science*, **251**, 283–287.

SCHREIBER, S. L., ALBERS, M. W. & BROWN, E. J. (1993). *Acc. Chem. Res.* **26**, 412–420.

SCHREIBER, S. L. & CRABTREE, G. R. (1992). *Immunol. Today*, **13**, 136–142.

SIEKIERKA, J. J., HUNG, S. H. Y., POE, M., LIN, C. S. & SIGAL, N. H. (1989). *Nature (London)*, **341**, 755–757.

SIGAL, N. H. & DUMONT, F. J. (1992). *Annu. Rev. Immunol.* **10**, 519–560.

SOMERS, P. K., WANDLESS, T. J. & SCHREIBER, S. L. (1991). *J. Am. Chem. Soc.* **113**, 8045–8056.

STUDIER, F. W. & MOFFATT, B. A. (1986). *J. Mol. Biol.* **189**, 113–130.

STUDIER, F. W., ROSENBERG, A. H., DUNN, J. J. & DUBENDORFF, J. W. (1990). *Methods Enzymol.* **185**, 60–89.

TOCCI, M. J., MATKOVICH, D. A., COLLIER, K. A., KWOK, P., DUMONT, F., LIN, S., DEGUDICIBUS, S., SIEKIERKA, J. J., CHIN, J. & HUTCHINSON, N. I. (1989). *J. Immunol.* **143**, 718–726.

VAN DUYNE, G. D., STANDAERT, R. F., KARPLUS, P. A., SCHREIBER, S. L. & CLARDY, J. (1991). *Science*, **252**, 839–842.

VAN DUYNE, G. D., STANDAERT, R. F., KARPLUS, P. A., SCHREIBER, S. L. & CLARDY, J. (1993). *J. Mol. Biol.* **229**, 105–124.

VAN DUYNE, G. D., STANDAERT, R. F., SCHREIBER, S. L. & CLARDY, J. (1991). *J. Am. Chem. Soc.* **113**, 7433–7434.

VEZINA, C., KUDELSKI, A. & SEHGAL, S. N. (1975). *J. Antibiot. (Tokyo)*, **28** 721–726.

WLODAWER, A & ERICKSON, J. W. (1993). *Annu. Rev. Biochem.* **62**, 543–585.

YANG, D., ROSEN, M. K. & SCHREIBER, S. L. (1993). *J. Am. Chem. Soc.* **115**, 819–820.